Int. J. Solids Structures, 1972, Vol. 8, pp. 111 to 129. Pergamon Press. Printed in Great Britain

TRANSIENT RESPONSE OF SUBMERGED SPHEROIDAL SHELLS

BEDROS BEDROSIAN and FRANK L. DIMAGGIO

Department of Civil Engineering and Engineering Mechanics,
Columbia University, New York, New York 10027

Abstract—The transient response of an elastic prolate spheroidal shell to a uniform pressure suddenly applied to its surface, and the pressure field in the surrounding acoustic fluid are obtained. By appropriate transformations of response functions and a geometric variable the problem is reduced to the simultaneous numerical integration, in a finite domain, of partial differential equations on functions which are regular in the space variables. An approximate relation is established to represent the fluid field, which, together with the plane wave approximation, is then used to obtain approximate solutions for the shell response. Extensive numerical results are presented for steel shells in sea water.

1. INTRODUCTION

THE extensional, steady-state response of submerged prolate spheroidal shells, and the accompanying sound field have been studied by Yen and DiMaggio [1].

By assuming that the fluid satisfies a plane wave equation (or making an equivalent assumption), Carrier [2], Mindlin and Bleich [3] and others obtained the transient response of submerged cylindrical shells for short times after the initiation of loading. Haywood [4] improved this approximation for cylindrical shells by using a fluid potential satisfying the cylindrical wave equation. The validity of these procedures has been discussed by Klosner [5].

In this paper, the extensional displacements of submerged prolate spheroidal shells and the pressure in the surrounding fluid, due to a uniform pressure of constant magnitude suddenly applied to the shell surface, are obtained by using suitable numerical techniques. First the tangential displacement is transformed such that the two regular singular points are eliminated from the differential equations governing the shell response. Then a transformation of the radial coordinate reduces the infinite physical domain into a (finite) rectangular mathematical one within which, and on the boundaries of which, all functions of interest are regular in the space variables. A numerical integration scheme appropriate to the resulting system of partial differential equations is then employed to obtain numerical results for a steel shell, with a major to minor axis ratio of six, submerged in sea water.

A spheroidal wave approximation is developed analogous to Haywood's cylindrical wave approximation [4]. It is shown that this approximation (and all the others mentioned) are valid either for the far field or short times. When the spheroidal wave approximation is combined with the plane wave approximation, the equations governing fluid and shell are uncoupled (as they are when the plane wave approximation is used alone). Numerical results for the shell displacements are obtained using each of these approximations and compared with those obtained using the more exact theory.

2. FORMULATION OF THE PROBLEM

Using Flammer's [6] notation, the prolate spheroidal coordinate system and geometry of the shell are shown in Figs. 1 and 2. The shell is assumed to be bounded by confocal spheroids defined by $\xi = a \pm h/d$, where d is the interfocal distance, h is the minimum thickness and $\xi = a$ (eccentricity is $1/a$) defines the middle surface. The displacements $w(\eta, t)$ and $u(\eta, t)$, respectively, perpendicular and tangent to the middle surface, are termed radial and tangential. Consistent with the thin shell theory that follows, an applied radial load $f(\eta, t)$ acts in the positive ξ direction at $\xi = a$ and an acoustic fluid occupies the space $\xi > a$.

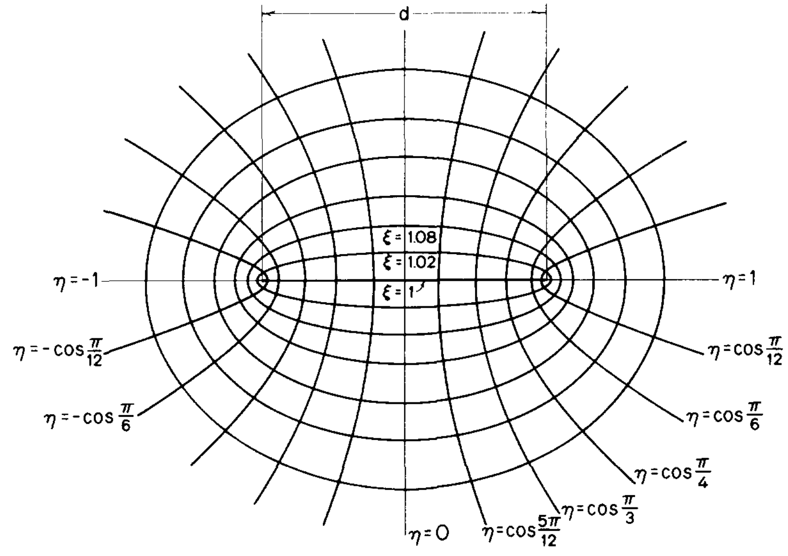

FIG. 1. Prolate spheroidal coordinate system.

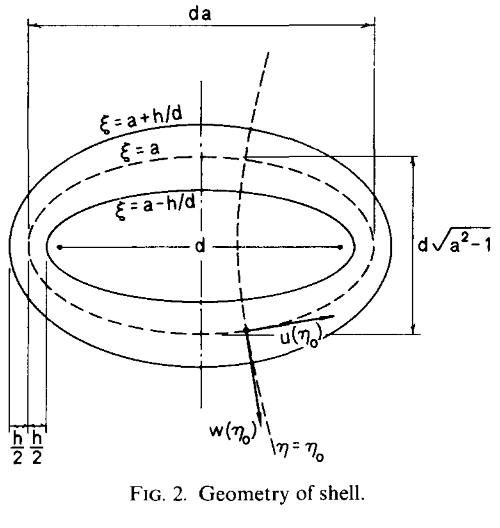

FIG. 2. Geometry of shell.

The extensional shell displacements satisfy the following equations:

$$L_{uu}u+L_{uw}w+(l/2c_s)^2M\ddot{u} = 0, \tag{1}$$

$$L_{wu}u+L_{ww}w+\left(\frac{l}{2c_s}\right)^2M\ddot{w} = \frac{l^2}{4\mu h}\left(\frac{a^2-1}{a^2-\eta^2}\right)^{\frac{1}{2}}M(f-p_a), \tag{2}$$

where dots denote differentiation with respect to time, and L_{uu}, etc., are differential operators:

$$L_{uu} = -(1-\eta^2)^{\frac{1}{2}}(\mathrm{d}^2/\mathrm{d}\eta^2)(1-\eta^2)^{\frac{1}{2}}-(1-\nu), \tag{3}$$

$$L_{uw} = -\left(\frac{1-\eta^2}{a^2-1}\right)^{\frac{1}{2}}\frac{\mathrm{d}}{\mathrm{d}\eta}\left[a\nu+\frac{a(a^2-1)}{a^2-\eta^2}\right]-\left(\frac{1-\eta^2}{a^2-1}\right)^{\frac{1}{2}}\frac{(1-\nu)a\eta}{a^2-\eta^2}, \tag{4}$$

$$L_{wu} = \left[a\nu+\frac{a(a^2-1)}{a^2-\eta^2}\right]\frac{\mathrm{d}}{\mathrm{d}\eta}\left(\frac{1-\eta^2}{a^2-1}\right)^{\frac{1}{2}}-\left(\frac{1-\eta^2}{a^2-1}\right)^{\frac{1}{2}}\frac{(1-\nu)a\eta}{a^2-\eta^2}, \tag{5}$$

and

$$L_{ww} = \frac{a^2}{a^2-1}+\frac{2\nu a^2}{a^2-\eta^2}+\frac{a^2(a^2-1)}{(a^2-\eta^2)^2}. \tag{6}$$

In these equations,

$$M = \tfrac{1}{2}(1-\nu)[(a^2-\eta^2)/a^2]; \tag{7}$$

l is the major axis of the shell middle surface (see Fig. 2);

$$c_s = (\mu/\rho_s)^{\frac{1}{2}}, \tag{8}$$

where μ is the shear modulus, ν is Poisson's ratio and ρ_s is the mass density of the shell material; and $p_a(\eta, t)$ is the fluid pressure on the shell surface, i.e.

$$p_a(\eta, t) = p(\xi, \eta, t)]_{\xi=a}. \tag{9}$$

The shell equations of motion, (1) and (2), may be derived through the application of Hamilton's principle, which also furnishes the natural boundary conditions:

$$u(\pm 1, t) = 0, \tag{10a}$$

$$w(\pm 1, t) \text{ is bounded.} \tag{10b}$$

The fluid velocity potential $\Phi(\xi, \eta, t)$ satisfies the wave equation

$$\nabla^2\Phi = (1/c^2)\ddot{\Phi}, \tag{11}$$

where c is the velocity of sound propagation in the fluid and the axisymmetric Laplacian in prolate spheroidal coordinates is

$$\nabla^2 = \left(\frac{2}{d}\right)^2\frac{1}{\xi^2-\eta^2}\left[\frac{\partial}{\partial\eta}(1-\eta^2)\frac{\partial}{\partial\eta}+\frac{\partial}{\partial\xi}(\xi^2-1)\frac{\partial}{\partial\xi}\right]. \tag{12}$$

The radial velocity of the shell must be equal to that of the fluid on its surface. Therefore,

$$\dot{w} = -(\partial\Phi/\partial n)]_{\xi=a}, \tag{13}$$

where the right-hand side is the normal directional derivative of the fluid velocity potential Φ.

Since

$$dn = h_\xi \, d\xi, \tag{14}$$

where the stretch ratio h_ξ in prolate spheroidal coordinates is

$$h_\xi = \tfrac{1}{2}d[(\xi^2-\eta^2)/(\xi^2-1)]^{\frac{1}{2}}, \tag{15}$$

equation (13) may be rewritten as

$$\dot{w} = -(1/h_\xi)(\partial\Phi/\partial\xi)]_{\xi=a}. \tag{16}$$

At some time ($t = 0$), a uniform radial pressure is suddenly applied on the shell surface. Then, in equation (2)

$$f(\eta, t) = -P_0 H(t), \tag{17}$$

where $H(t)$ is the Heaviside step function.

The fluid velocity potential and the fluid pressure are related through:

$$p = \rho\dot{\Phi}. \tag{18}$$

The shell and the acoustic fluid are assumed to be initially at rest, and the fluid pressure nil; thus, using equation (18):

$$u(\eta, 0) = w(\eta, 0) = \dot{u}(\eta, 0) = \dot{w}(\eta, 0) = 0, \tag{19}$$

$$\dot{\Phi}(\xi, \eta, 0) = 0. \tag{20}$$

Since the fluid potential need be determined only to an arbitrary constant, set

$$\Phi(\xi, \eta, 0) = 0. \tag{21}$$

To represent an outgoing wave, it must be required that [7]:

$$\lim_{r\to\infty} [(\partial\Phi/\partial r)+(1/c)\dot{\Phi}] = 0(1/r), \tag{22}$$

where r is the radial distance from the shell center. Since

$$\lim_{r\to\infty} r = \lim_{\xi\to\infty} \tfrac{1}{2}\,d\xi, \tag{23}$$

as may be readily seen from Fig. 1, equation (22) may be written as:

$$\lim_{\xi\to\infty} [(2/d)(\partial\Phi/\partial\xi)+(1/c)\dot{\Phi}] = 0(1/\xi) \tag{24}$$

It is now required to determine functions $u(\eta, t)$, $w(\eta, t)$ and $\Phi(\xi, \eta, t)$ such that equations (1), (2), (10), (11), (16), (19)–(21) and (24) are satisfied.

3. REMOVAL OF SINGULARITIES AND TRANSFORMATION OF DOMAIN

Solutions of equation (11) that satisfy equation (24) have the form

$$\Phi(\xi, \eta, t) = D\left(\eta, t-\frac{d}{2}\frac{\xi}{c}\right) \Big/ \xi, \tag{25}$$

where $D[\eta, t-(d/2)(\xi/c)]$ is regular in ξ and η in the region $\xi > a$, $-1 \le \eta \le +1$. This can be written as

$$\Phi(\xi, \eta, t) = (1-\eta^2)^{-1}G(\xi, \eta, t), \quad (26)$$

where

$$G(\xi, \eta, t) = (1-\eta^2)\left[D\left(\eta, t-\frac{d}{2}\frac{\xi}{c}\right) \Big/ \xi\right] \quad (27)$$

is regular in ξ and η in the region $\xi > a$, $-1 \le \eta \le +1$.

Assuming that $f(\eta, t)$ is regular in η, it follows from equations (1), (2), (16) and (18) that $w(\eta, t)$ is regular in η and that

$$u(\eta, t) = (1-\eta^2)^{-\frac{1}{2}}S(\eta, t), \quad (28)$$

where $S(\eta, t)$ is regular in η and, using equation (10a),

$$S(\pm 1, t) = 0. \quad (29)$$

Letting

$$w(\eta, t) = (1-\eta^2)^{-1}Z(\eta, t), \quad (30)$$

where $Z(\eta, t)$ is regular in η and using equation (10b),

$$Z(\pm 1, t) = 0. \quad (31)$$

To map the infinite physical domain $\xi \ge a$, $-1 \le \eta \le +1$, onto the finite mathematical domain $0 \le y \le 1$, $-1 \le \eta \le +1$, let

$$y = 1/(e\xi), \quad (32)$$

where

$$e = 1/a \quad (33)$$

is the eccentricity of the shell middle surface. Then, instead of equation (26) the form of the fluid velocity potential becomes

$$(1-\eta^2)^{-1}F(y, \eta, t), \quad (34)$$

where, from equation (27), F is regular in y and η and satisfies

$$F(0, \eta, t) = 0, \quad (35)$$

$$F(y, \pm 1, t) = 0. \quad (36)$$

If equations (28), (30) and (34) are substituted into equations (1), (2), (11), (16), (19), (21) and (20), these equations become, respectively,

$$f_1(\mathrm{d}^2S/\mathrm{d}\eta^2)+f_2S+f_3(\mathrm{d}Z/\mathrm{d}\eta)+f_4Z+f_5\ddot{S} = 0, \quad (37)$$

$$g_1(\mathrm{d}S/\mathrm{d}\eta)+g_2S+g_3Z+g_4\ddot{Z} = g_5\dot{F}]_{y=1}+g_6, \quad (38)$$

$$h_1\ddot{F} = h_2(\partial^2F/\partial y^2)+h_3(\partial^2F/\partial\eta^2)+h_4(\partial F/\partial y)+h_5(\partial F/\partial\eta)+h_6F, \quad (39)$$

$$\left(\frac{2}{l}\right)\left(\frac{a^2-1}{a^2-\eta^2}\right)^{\frac{1}{2}}\frac{\partial F}{\partial y}\Bigg]_{y=1} = \dot{Z}, \quad (40)$$

$$S(\eta, 0) = Z(\eta, 0) = \dot{S}(\eta, 0) = \dot{Z}(\eta, 0) = 0, \quad (41)$$

$$F(y, \eta, 0) = 0, \quad (42)$$

and

$$\dot{F}(y, \eta, 0) = 0, \tag{43}$$

where the functions f_1–f_5, g_1–g_6 and h_1–h_6, of η or η and y are written out in Appendix A.

The problem of solving equations (1), (2), (10), (11), (16), (19)–(21) and (24) for the functions $\Phi(\xi, \eta, t)$ and $w(\eta, t)$ which are regular in ξ and η, and $u(\eta, t)$, which has regular singular points at $\eta = \pm 1$, in the infinite physical domain $\xi \geq a$, $-1 \leq \eta \leq +1$, has been transformed into the problem of solving equations (37)–(43), (29), (31), (35) and (36) on the functions $F(y, \eta, t)$, $Z(\eta, t)$ and $S(\eta, t)$, which are regular in y and η, in the finite mathematical domain $0 \leq y \leq 1$, $-1 \leq \eta \leq +1$, thus making numerical integration possible.

The transformation of the problem is illustrated in Figs. 3(a) and (b).

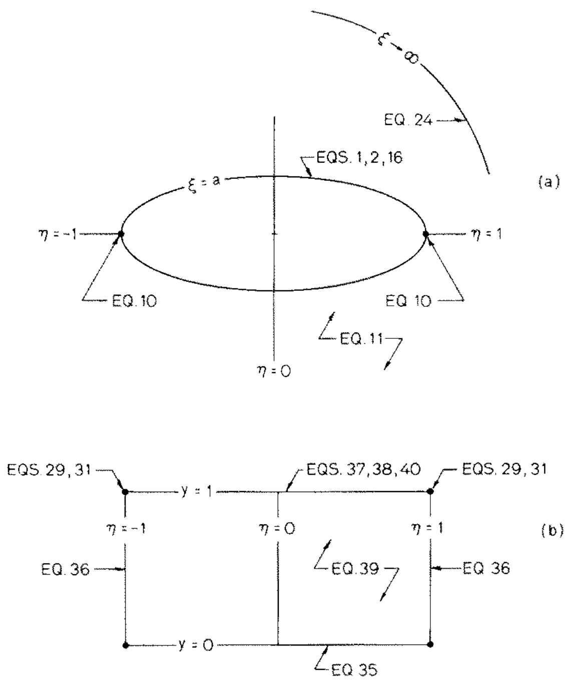

FIG. 3. (a) Physical domain and governing equations. (b) Transformed domain and governing equations.

For loads f symmetric in η, the displacement w is symmetric in η while the displacement u and the $\eta-$ component of the fluid velocity are antisymmetric in η. Therefore,

$$w(\eta, t) = w(-\eta, t), \tag{44}$$

$$u(\eta, t) = -u(-\eta, t), \tag{45}$$

and

$$(1/h_\eta)(\partial\Phi/\partial\eta)]_{+\eta} = -(1/h_\eta)(\partial\Phi/\partial\eta)]_{-\eta}, \tag{46}$$

where the stretch ratio h_η in prolate spheroidal coordinates is

$$h_\eta = \tfrac{1}{2}d[(\xi^2-\eta^2)/(1-\eta^2)]^{\frac{1}{2}}, \tag{47}$$

or, as may be seen from equations (30), (28) and (34),

$$Z(\eta, t) = Z(-\eta, t), \tag{48}$$

$$S(\eta, t) = -S(-\eta, t), \tag{49}$$

and

$$F(y, \eta, t) = F(y, -\eta, t) \tag{50a}$$

$$(\partial F/\partial \eta)]_{+\eta} = -(\partial F/\partial \eta)]_{-\eta}. \tag{50b}$$

Similarly, for antisymmetric applied loads,

$$Z(\eta, t) = -Z(-\eta, t), \tag{51}$$

$$S(\eta, t) = S(-\eta, t), \tag{52}$$

and

$$F(y, \eta, t) = -F(y, -\eta, t) \tag{53a}$$

$$(\partial F/\partial \eta)]_{+\eta} = (\partial F/\partial \eta)]_{-\eta}. \tag{53b}$$

By making use of equations (48)–(50), (51)–(53), as appropriate, only half the domain of Fig. 3(b), i.e. $0 \leq \eta \leq +1$, need be considered.

4. NUMERICAL INTEGRATION

To solve this mixed initial boundary value problem, the square region $0 \leq \eta \leq 1$, $0 \leq y \leq 1$ of Fig. 3(b) is subdivided into a grid with N subdivisions in both the η and y coordinates with spacing

$$\delta = 1/N. \tag{54}$$

In equations (38) and (40) the space derivatives are replaced by difference expressions with errors of order δ^2, and difference expressions with errors of the order of the square of the time step are used for the time derivatives. This transforms the differential equations (38) and (40) into recurrence equations of the explicit type involving the values of the unknown functions at time t_i and at two preceding time steps, t_{i-1} and t_{i-2}, at the pivotal points $(y_N, \eta_0) \ldots (y_N, \eta_{N-1})$ shown in Fig. 4. To obtain a stable finite difference scheme to approximate equation (37), von Neumann's finite difference method [8] is used. The resulting difference equations are of the implicit type and their solution requires the inversion of a linear system of $N-1$ algebraic equations in the same number of unknowns at each time step. The matrix of the coefficients of the unknown pivotal values $S_{Nj}(t_i), j = 1 \ldots (N-1)$, has a tri-diagonal form, making application of the classical Gaussian algorithm of elimination—back substitution quite efficient. Finally, use of the alternating-direction method [9] on the differential equation (39) governing the fluid response transforms it into recurrence equations of the implicit type involving the unknown pivotal values at time t_i and at two preceding time steps at the pivotal points shown in Fig. 4. The matrix of the coefficients of the resulting algebraic equations has a tri-diagonal form and the Gaussian algorithm is

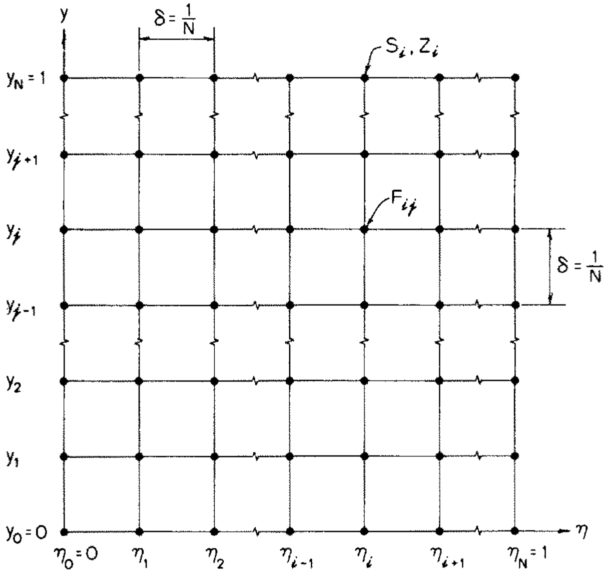

FIG. 4. Grid system used for numerical integration.

again appropriate. For a given shell and applied pressure, a typical solution for the shell displacements and fluid pressure field took approximately 1·7 min for $N = 10$ on an IBM-360/91 computer.

5. APPROXIMATE SOLUTIONS

Approximate expressions for the elastic wave equation, equation (11), governing the acoustic fluid field were used to find the transient response of a cylindrical shell by Carrier [2], Mindlin and Bleich [3] and by Haywood [4]. Similar expressions which approximate the acoustic fluid field, valid for short times after load application, may be used to obtain approximate solutions for the spheroidal shell response. These expressions, derived in Appendix B, are the plane wave approximation (P.W.A.)

$$\frac{\partial \Phi}{\partial[\xi(d/2)]} = -\frac{1}{c}\dot{\Phi}, \tag{55}$$

and the spheroidal wave approximation (Sp.W.A.)

$$\frac{\partial \dot{\Phi}}{\partial[\xi(d/2)]} = -\frac{1}{c}\dot{\Phi} - \frac{1}{[\xi(d/2)]}\Phi. \tag{56}$$

Plane wave approximation (P.W.A.)

From equation (18), using equations (15), (16) and the plane wave approximation, equation (55), one obtains

$$p_a = \rho c[(a^2 - \eta^2)/(a^2 - 1)]^{\frac{1}{2}}\dot{w}, \tag{57}$$

which substituted into equation (2) uncouples the equations governing the shell and fluid responses.

The shell response may now be obtained from equations (1), (2), (10) and (19), with the aid of equation (57). Assuming that $f(\eta, t)$ is regular in η it follows that $w(\eta, t)$ is regular in η and that

$$u(\eta, t) = (1 - \eta^2)^{-\frac{1}{2}} S(\eta, t), \tag{28}$$

where $S(\eta, t)$ is regular in η. Let

$$w(\eta, t) = (1 - \eta^2)^{-1} Z(\eta, t), \tag{30}$$

where $Z(\eta, t)$ is regular in η.

The problem of solving for the functions $w(\eta, t)$, regular in η and $u(\eta, t)$, with regular singular points at $\eta = \pm 1$, from the equations (1), (2), (10), (19) and (57), has been transformed into the problem of solving for the functions $S(\eta, t)$ and $Z(\eta, t)$, regular in η, from the following equations, respectively:

$$f_1(\mathrm{d}^2S/\mathrm{d}\eta^2) + f_2 S + f_3(\mathrm{d}Z/\mathrm{d}\eta) + f_4 Z + f_5 \ddot{S} = 0, \tag{37}$$

$$g_1(\mathrm{d}S/\mathrm{d}\eta) + g_2 S + g_3 Z + g_4 \ddot{Z} + g_5^p \dot{Z} = g_6, \tag{58}$$

$$S(\pm 1, t) = 0, \tag{29}$$

$$Z(\pm 1, t) = 0, \tag{31}$$

and

$$S(\eta, 0) = Z(\eta, 0) = \dot{S}(\eta, 0) = \dot{Z}(\eta, 0) = 0, \tag{41}$$

where

$$g_5^p(\eta) = -c[(a^2 - \eta^2)/(a^2 - 1)]^{\frac{1}{2}} g_5(\eta), \tag{59}$$

and the functions f_1–f_5 and g_1–g_6 of η were previously defined. Numerical integration is now possible (see Section 4).

Spheroidal wave approximation (*Sp.W.A.*)

If equation (56) is used to represent the acoustic fluid field, then, from equations (18), (15), (16) and (56), one obtains:

$$p_a = \rho c[(a^2 - \eta^2)/(a^2 - 1)]^{\frac{1}{2}} \dot{w} - \rho c(2/l)\Phi]_{\xi = a}. \tag{60}$$

As may be seen from equations (2), (60), (56) and (16), the spheroidal wave approximation, although considerably simplifying the problem of numerical integration, does not uncouple the equations governing the shell and fluid responses. Using equations (28), (30), (34) and (32), the problem of solving for the functions $\Phi(\xi, \eta, t)$ and $w(\eta, t)$, which are regular in ξ and η, and $u(\eta, t)$, which has regular singular points at $\eta = \pm 1$, in the infinite physical domain $\xi \geq a$, $1 \leq \eta \leq +1$, from the equations (1), (2), (10), (56), (16), (19), (20), (21) and (24), is transformed into the problem of solving for the functions $F(y, \eta, t)$, $Z(\eta, t)$ and $S(\eta, t)$, which are regular in y and η, in the finite mathematical domain $0 \leq y \leq 1$, $-1 \leq \eta \leq +1$, thus making numerical integration possible, from the equations (37), (38), (40)–(43), (29), (31), (35), (36) and

$$j_1(\partial F/\partial y) + j_2 F + j_3 \dot{F} = 0, \tag{61}$$

where

$$j_1(y) = -y^2, \quad (62a)$$

$$j_2(y) = y, \quad (62b)$$

and

$$j_3 = (1/c)(l/2). \quad (62c)$$

Since both plane and spheroidal wave approximations are valid for short times, the equations governing the shell and fluid responses may be uncoupled by using equations (55), (15), (16), (19) and (21) to approximate the second term on the right side of equation (60), which then becomes

$$p_a = \rho c[(a^2-\eta^2)/(a^2-1)]^{\frac{1}{2}}\dot{w} - \rho c^2(2/l)[(a^2-\eta^2)/(a^2-1)]^{\frac{1}{2}}w. \quad (63)$$

Thus, the problem of solving for the function $w(\eta, t)$, regular in η, and $u(\eta, t)$, with regular singular points at $\eta = \pm 1$, from equations (1), (2), (10), (19) and (63), is transformed into the problem of solving for the functions $S(\eta, t)$ and $Z(\eta, t)$, regular in η, from the following equations

$$f_1(\mathrm{d}^2S/\mathrm{d}\eta^2)+f_2S+f_3(\mathrm{d}Z/\mathrm{d}\eta)+f_4Z+f_5\ddot{S} = 0, \quad (37)$$

$$g_1(\mathrm{d}S/\mathrm{d}\eta)+g_2S+g_3^SZ+g_4\ddot{Z}+g_5^p\dot{Z} = g_6, \quad (64)$$

$$S(\pm 1, t) = 0, \quad (29)$$

$$Z(\pm 1, t) = 0, \quad (31)$$

and

$$S(\eta, 0) = Z(\eta, 0) = \dot{S}(\eta, 0) = \dot{Z}(\eta, 0) = 0, \quad (41)$$

where $S(\eta, t)$ and $Z(\eta, t)$ are defined in equations (28) and (30),

$$g_3^S(\eta) = g_3(\eta)+c^2(2/l)[(a^2-\eta^2)/(a^2-1)]^{\frac{1}{2}}g_5(\eta), \quad (65)$$

and the functions f_1–f_5, g_1–g_6 and g_5^p of η were previously defined. Numerical integration may now be used.

6. EXACT SOLUTION FOR SPHERICAL SHELL

If equations (2), (10b), (11), (16), (19)–(21) and (24) are written for spherical geometry, the transient response of the spherical shell immersed in an acoustic fluid due to a uniform radial pressure, P_0, suddenly applied on the shell surface, and the corresponding fluid pressure field are obtained, respectively, as

$$w(t) = w_{ST}\left[1-\frac{4(1+\nu)}{1-\nu}\left(\frac{c_s}{c}\right)^2\sum_{i=1}^{3}\frac{1+\alpha_i}{\left(1+\frac{R_0}{h}\frac{\rho}{\rho_s}\right)\alpha_i^2+\frac{8(1+\nu)}{6-\nu}\left(\frac{c_s}{c}\right)^2\alpha_i+\frac{12(1+\nu)}{1-\nu}\left(\frac{c_s}{c}\right)^2}\right.$$
$$\left.\times\, \mathrm{e}^{\alpha_i(c/R_0)t}\right]H(t), \quad (66)$$

and

$$p(R,t)\begin{cases} = -\dfrac{R_0}{R}\dfrac{R_0}{h}\dfrac{\rho}{\rho_s}P_0\left\{\displaystyle\sum_{i=1}^{3}\frac{\alpha_i^2}{2\alpha_i^3+\left(1+\dfrac{R_0}{h}\dfrac{\rho}{\rho_s}\right)\alpha_i^2-\dfrac{4(1+\nu)}{1-\nu}\left(\dfrac{c_s}{c}\right)^2}\right. \\ \left.\quad\times\, e^{\alpha_i[ct-(R-R_0)]/R_0}\right\}, \quad \text{for } (R-R_0)<ct, \\ = 0, \quad \text{for } (R-R_0)\geq ct. \end{cases} \tag{67}$$

The shell response of equation (66) has been previously displayed by Klosner and Lou [10]. In these equations R_0 is the radius of the shell middle-surface, R is the radial distance from the shell center, h is the shell thickness, w_{ST} is the static radial displacement (assumed positive outward) under the uniform radial pressure P_0,

$$w_{ST} = -\frac{R_0^2}{h}\frac{P_0}{E}\frac{6-\nu}{2}, \tag{68}$$

and α_i $(i = 1, 2, 3)$ are the roots of the algebraic equation:

$$x^3+\left(1+\frac{R_0}{h}\frac{\rho}{\rho_s}\right)x^2+\frac{4(1+\nu)}{1-\nu}\left(\frac{c_s}{c}\right)^2 x+\frac{4(1-\nu)}{1-\nu}\left(\frac{c_s}{c}\right)^2 = 0. \tag{69}$$

Equations (66) or (67) may be used to check the numerical integration scheme discussed in Section 4 for $e = 0$ and $l = R_0$.

7. NUMERICAL EXAMPLES

The calculations were performed using the following material constants and shell geometry:

$$\nu = 0{\cdot}30,$$

$$c_s = 1{\cdot}232\times10^5 \text{ in./sec},$$

$$c = 0{\cdot}590\times10^5 \text{ in./sec},$$

$$\rho_s = 0{\cdot}7345\times10^{-3} \text{ lb}\times\text{sec}^2/\text{in.}^4,$$

$$\rho = 0{\cdot}9582\times10^{-4} \text{ lb}\times\text{sec}^2/\text{in.}^4,$$

$$l = 42 \text{ in.},$$

$$h = 0{\cdot}40 \text{ in.},$$

which correspond to a thin steel shell in sea water.

The numerical procedure developed in Section 4 for the exact formulation was first applied using a 10×10 grid ($N = 10$) to a spherical shell ($e = 0$), to which a uniform pressure P_0 is suddenly applied, and compared with the exact solution of equation (66). The results of these calculations are illustrated in Fig. 5 for the radial shell response at $\eta = 0$. The agreement between the exact solutions and those obtained by the numerical technique outlined in Section 4 is seen to be good.

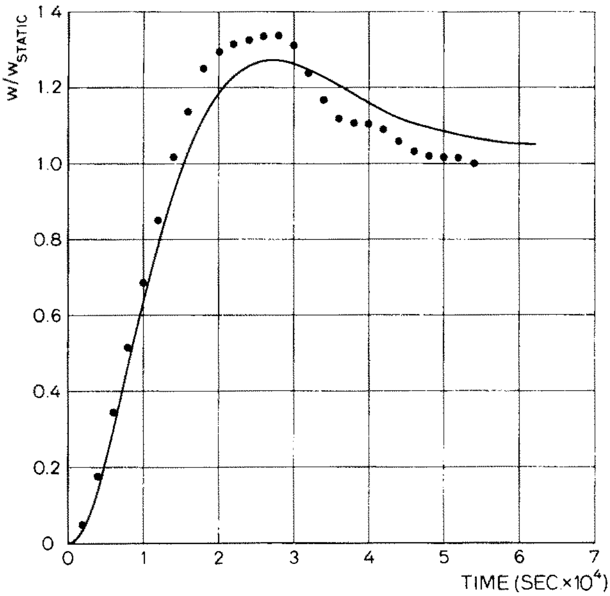

FIG. 5. Comparison of radial response of spherical shell at $\eta = 0$ obtained from the exact solution (———) and from numerical integration (●).

The equations were then integrated numerically for a spheroidal shell with ratio of major to minor axis equal to 6 ($e = 0{\cdot}986$), with a uniform pressure envelope P_0 suddenly applied to the shell middle-surface, using $N = 10$ and the procedure outlined in Section 4. Some of the results are plotted in Figs. 6–8. For the shell chosen the radial displacement

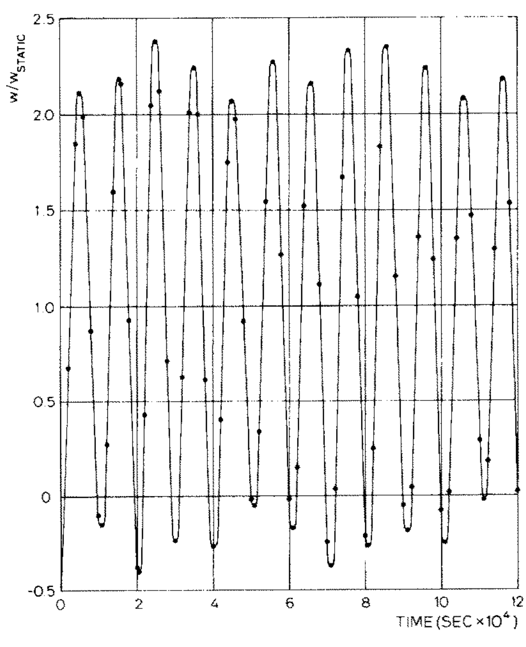

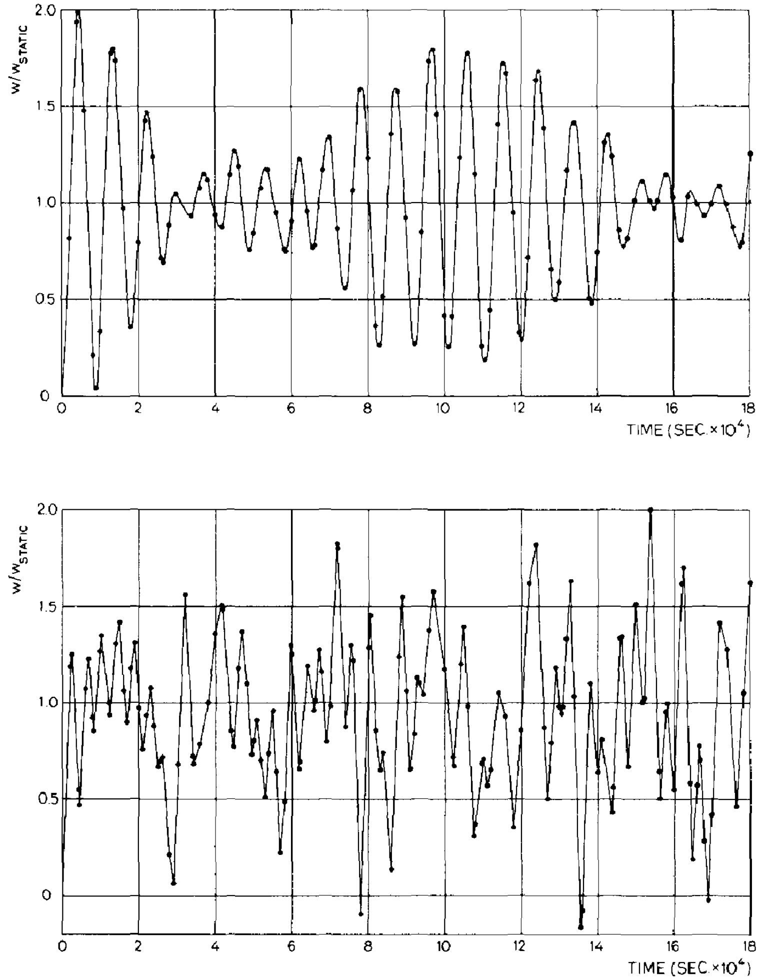

FIG. 6. Radial displacement response of spheroidal shell, $e = 0{\cdot}986$, at (a) $\eta = 0$, (b) $\eta = 0{\cdot}5$ and (c) $\eta = 0{\cdot}9$.

at $\eta = 0$ displayed in Fig. 6(a) shows little damping and slightly visible beating, while in Fig. 6(b), displaying the radial displacement at $\eta = 0{\cdot}5$, the beating phenomenon is pronounced. The radial displacement at $\eta = 0{\cdot}9$ is exhibited in Fig. 6(c). In Figs. 7(a)–(c) the fluid pressure time history at three points at the shell surface ($y = 1{\cdot}0$) are shown. The far field pressure amplitude distribution exhibited in Fig. 8 shows almost no directivity.

Approximate solutions for the spheroidal shell response were obtained using the coupled spheroidal, the uncoupled spheroidal and the plane wave approximation formulations. The results are displayed in Figs. 9(a)–(c) and compared with the numerical solution of the exact formulation. The numerical solution for the shell displacements using the coupled spheroidal wave approximation formulation took approximately 0·5 min for $N = 10$ on an IBM-360/91 computer and for the early stages of the motion gives results in

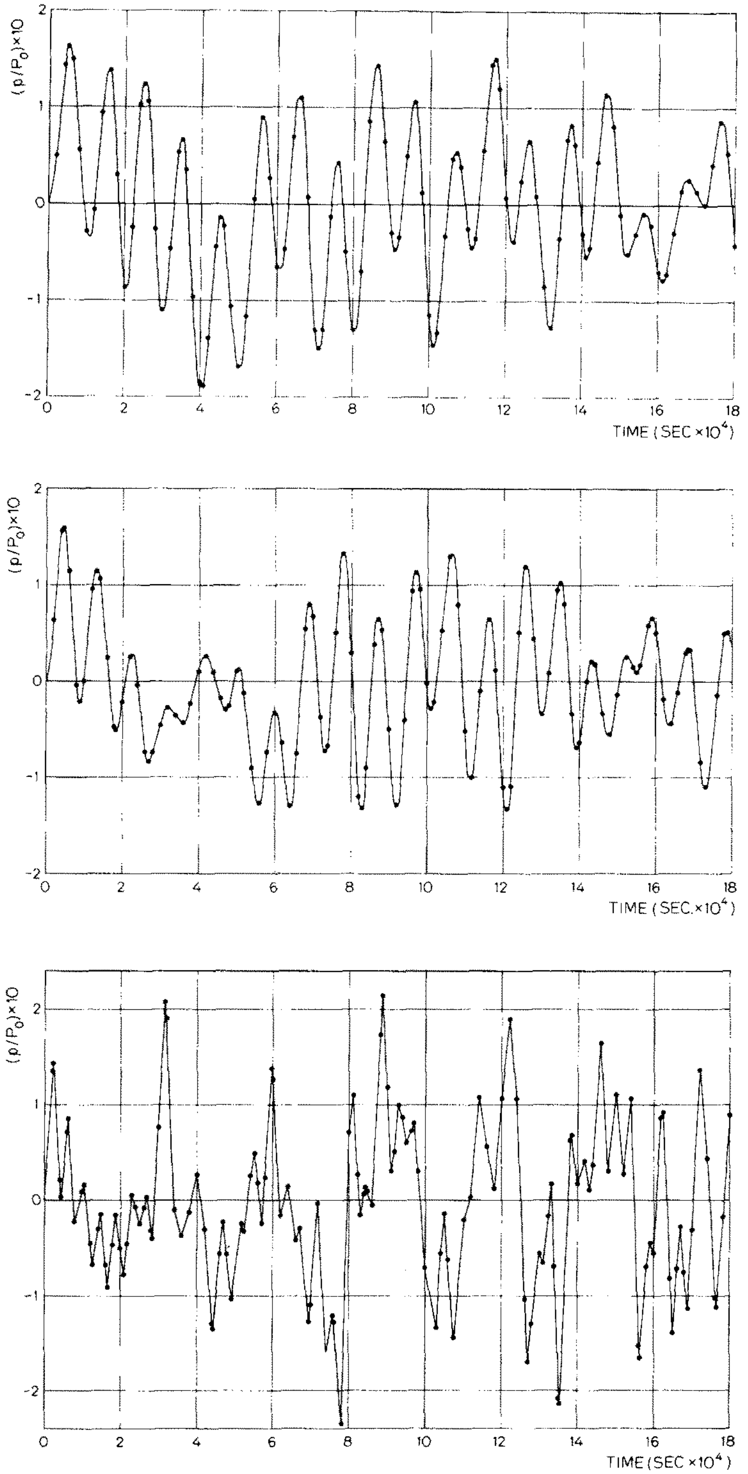

FIG. 7. Surface pressure response for spheroidal shell, $e = 0{\cdot}986$, at (a) $\eta = 0$, (b) $\eta = 0{\cdot}5$ and (c) $\eta = 0{\cdot}9$.

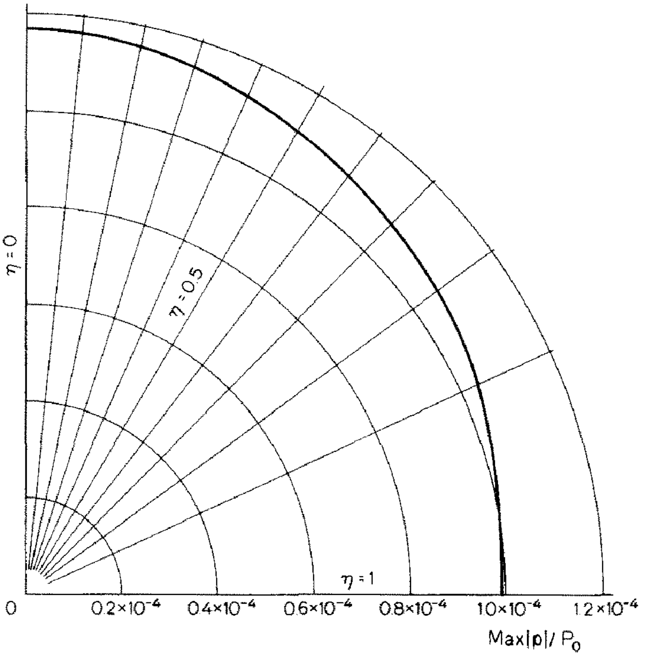

FIG. 8. Farfield (y = 0·20) pressure amplitude distribution for spheroidal shell, e = 0·986.

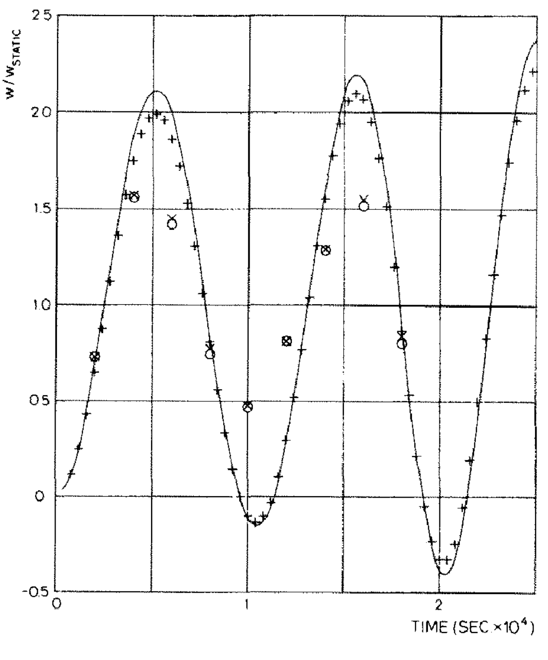

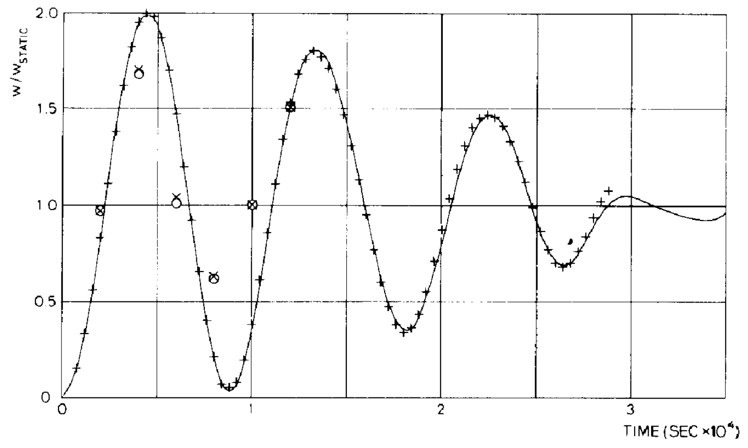

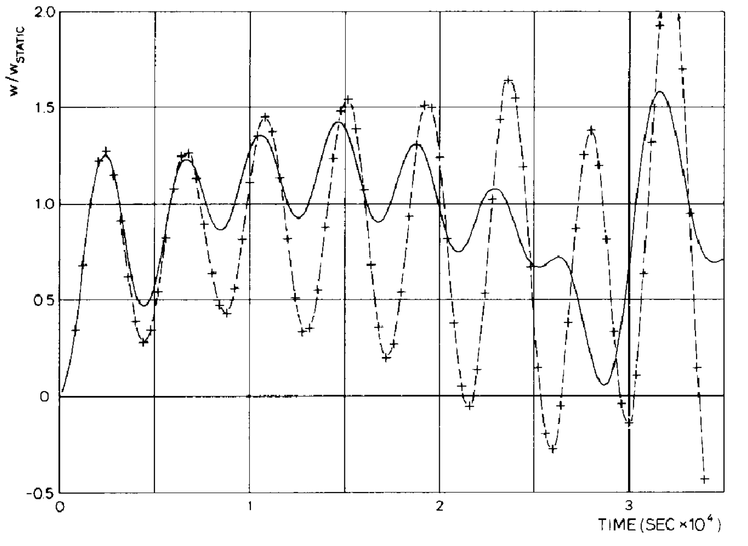

FIG. 9. Comparison of radial response of spheroidal shell, $e = 0{\cdot}986$, at (a) $\eta = 0$, (b) $\eta = 0{\cdot}5$ and (c) $\eta = 0{\cdot}9$ obtained from numerical integration of the exact formulation (———), of the coupled spheroidal wave approximation (+), of the uncoupled spheroidal wave approximation (×) and of the plane wave approximation (○).

very good agreement with the numerical solution of the exact formulation which took approximately 1·7 min on the same computer.

The numerical solutions for the shell displacements obtained using the uncoupled spheroidal wave approximation and the plane wave approximation for the same shell took less computing time but did not provide good agreement with the numerical solution of the exact formulation.

REFERENCES

[1] T. YEN and F. DIMAGGIO, Forced vibrations of submerged spheroidal shells. *J. acoust. Soc. Am.* **41**, 618–626 (1967).

[2] G. F. CARRIER, The Response of a Submerged Cylindrical Shell to an Axially Propagating Acoustic Wave, Brown University Technical Report No. 19, Contract N7 onr-35810 (1953).

[3] R. D. MINDLIN and H. H. BLEICH, Response of an elastic cylindrical shell to a transverse, step shock wave. *J. appl. Mech.* **20**, 189–195 (1953), *Trans. Am. Soc. Mech. Engrs* **75**, 189–195 (1953).

[4] J. H. HAYWOOD, Response of an elastic cylindrical shell to a pressure pulse. *Q. Jl Mech. appl. Math.* **11**, Part 2, 129–141 (1958).

[5] J. M. KLOSNER, Inadequacies of piston theory in fluid-shell interactions. *J. Engng Mech. Div. Am. Soc. civ. Engrs* **96**, 143–159 (1970).

[6] C. FLAMMER, *Spheroidal Wave Functions*. Stanford University Press (1957).

[7] A. N. TYCHONOV and A. A. SAMARSKI, *Partial Differential Equations of Mathematical Physics*, Vol. II, chapter 7, pp. 480–481. Holden-Day (1967).

[8] M. LEES, Von Neumann difference approximation to hyperbolic equations. *Pacific J. Math.* **10**, 213–222 (1960).

[9] M. LEES, Alternating direction methods for hyperbolic differential equations. *J. Soc. ind. appl. Math.* **10**, 610–616 (1962).

[10] Y. K. LOU and J. M. KLOSNER, Dynamics of a Submerged Ring-Stiffened Spherical Shell, Paper No. 70-WA/APM-42, Presented at the ASME Winter Annual Meeting, New York (1970).

APPENDIX A

$$f_1(\eta) = -(1-\eta^2)^2, \tag{A1}$$

$$f_2(\eta) = -(1-\nu)(1-\eta^2), \tag{A2}$$

$$f_3(\eta) = -\frac{a}{(a^2-1)^{\frac{1}{2}}}\frac{(1-\eta^2)}{(a^2-\eta^2)}[\nu(a^2-\eta^2)+(a^2-1)], \tag{A3}$$

$$f_4(\eta) = -\frac{a}{(a^2-1)^{\frac{1}{2}}}\frac{\eta}{(a^2-\eta^2)^2}\{(1+\nu)\eta^4-[(3\nu+5)a^2-(3+\nu)]\eta^2 + [2(1+\nu)a^4+(1-\nu)a^2-2]\}, \tag{A4}$$

$$f_5(\eta) = \left(\frac{l}{2c_s}\right)^2\left(\frac{1-\nu}{2}\right)\frac{1}{a^2}(a^2-\eta^2)(1-\eta^2), \tag{A5}$$

$$g_1(\eta) = \frac{a}{(a^2-1)^{\frac{1}{2}}}\frac{(1-\eta^2)}{(a^2-\eta^2)}[\nu(a^2-\eta^2)+(a^2-1)], \tag{A6}$$

$$g_2(\eta) = -\frac{a}{(a^2-1)^{\frac{1}{2}}}(1-\nu)\frac{\eta(1-\eta^2)}{(a^2-\eta^2)}, \tag{A7}$$

$$g_3(\eta) = a^2\left[\frac{1}{a^2-1}+\frac{2\nu}{a^2-\eta^2}+\frac{a^2-1}{(a^2-\eta^2)^2}\right], \tag{A8}$$

$$g_4(\eta) = \left(\frac{l}{2c_s}\right)^2\left(\frac{1-\nu}{2}\right)\frac{1}{a^2}(a^2-\eta^2), \tag{A9}$$

$$g_5(\eta) = -\frac{l^2}{4\mu h}\left(\frac{1-\nu}{2}\right)\frac{(a^2-1)^{\frac{1}{2}}}{a^2}\rho(a^2-\eta^2)^{\frac{1}{2}}, \tag{A10}$$

$$g_6(\eta) = -\frac{l^2}{4\mu h}\left(\frac{1-\nu}{2}\right)\frac{(a^2-1)^{\frac{1}{2}}}{a^2}P_0(a^2-\eta^2)^{\frac{1}{2}}(1-\eta^2)H(t); \tag{A11}$$

$$h_1(y,\eta) = \frac{1}{c^2}(1-\eta^2)(a^2-y^2\eta^2), \tag{A12}$$

$$h_2(y,\eta) = \left(\frac{2}{l}\right)^2 y^4(a^2-y^2)(1-\eta^2), \tag{A13}$$

$$h_3(y,\eta) = \left(\frac{2}{d}\right)^2 y^2(1-\eta^2)^2, \tag{A14}$$

$$h_4(y,\eta) = -2\left(\frac{2}{l}\right)^2 y^5(1-\eta^2), \tag{A15}$$

$$h_5(y,\eta) = 2\left(\frac{2}{d}\right)^2 y^2\eta(1-\eta^2), \tag{A16}$$

$$h_6(y,\eta) = 2\left(\frac{2}{d}\right)^2 y^2(1+\eta^2). \tag{A17}$$

APPENDIX B

Derivation of spheroidal wave approximation (Sp.W.A.)

The fluid velocity potential function, $\Phi(\eta, \varphi, \xi, t)$, satisfies the wave equation:

$$\nabla^2\Phi = \frac{1}{c^2}\ddot{\Phi} \tag{B1}$$

where the Laplacian in prolate spheroidal coordinates is

$$\nabla^2 = \left(\frac{2}{d}\right)^2 \frac{1}{\xi^2-\eta^2}\left[\frac{\partial}{\partial\eta}(1-\eta^2)\frac{\partial}{\partial\eta}+\frac{\partial}{\partial\xi}(\xi^2-1)\frac{\partial}{\partial\xi}+\frac{\xi^2-\eta^2}{(\xi^2-1)(1-\eta^2)}\frac{\partial^2}{\partial\varphi^2}\right]. \tag{B2}$$

Using Laplace's transform equation (B1) becomes:

$$\left[\nabla^2-\left(\frac{s}{c}\right)^2\right]\tilde{\Phi} = 0. \tag{B3}$$

Solutions to equation (B3) may be obtained in the form of Lamé products (Ref. 6, p. 11):

$$\tilde{\Phi}(\eta,\varphi,\xi,s) = \sum_{m,n=0}^{\infty} C_{mn}(s)S_{mn}\left(-i\frac{s}{c}\frac{d}{2},\eta\right)R_{mn}\left(-i\frac{s}{c}\frac{d}{2},\xi\right)\begin{matrix}\cos\\ \sin\end{matrix}(m\varphi), \tag{B4}$$

where S_{mn} and R_{mn} are, respectively, the angular and radial spheroidal wave functions.

For axisymmetric loading $\tilde{\Phi}$ must be independent of φ and requires $m = 0$.

Then equation (B4) becomes

$$\tilde{\Phi}(\eta,\xi,s) = \sum_{n=0}^{\infty} C_{0n}(s)S_{0n}\left(-i\frac{s}{c}\frac{d}{2},\eta\right)R_{0n}\left(-i\frac{s}{c}\frac{d}{2},\xi\right). \tag{B5}$$

Using asymptotic expansions for the radial functions R_{0n} (see for example Ref. 6, p. 67) valid for short times after load application and/or for the far field which also satisfy the condition for bounded $\tilde{\Phi}$, one obtains from equation (B5):

$$\tilde{\Phi}(\eta, \xi, s) = G(\eta, s)\frac{e^{-[(s/c)(d/2)]\xi}}{(s/c)(d/2)\xi}. \tag{B6}$$

From equation (B6) it follows that

$$\frac{\partial\tilde{\Phi}}{\partial\xi} = \left[-\frac{1}{\xi} - \frac{s}{c}\frac{d}{2}\right]\tilde{\Phi}. \tag{B7}$$

The inversion of equation (B7) yields the approximate spheroidal wave field equation:

$$\frac{\partial\Phi}{\partial[\xi(d/2)]} = -\frac{1}{c}\dot{\Phi} - \frac{1}{[\xi(d/2)]}\Phi. \tag{B8}$$

If the first term on the right side of (B7) is neglected, i.e. when $1/\xi \ll (s/c)(d/2)$, one obtains the plane wave approximation:

$$\frac{\partial\Phi}{\partial[\xi(d/2)]} = -\frac{1}{c}\dot{\Phi}. \tag{B9}$$

It should be noted that a similar procedure is possible for the nonaxisymmetric case.

(*Received* 25 *February* 1971)

Абстракт—Исследуется нестационарное поведение упругой, удлиненной, сферической оболочки, под влиянием равномерного давления, приложенного внезапно на ее поверхности, а также поле давления в окресмности акустической жидкости. Путем надлежащих преобразований функции поведения и геометрической переменной, задача сводится к одновременному численному интегрированию, в конечной области, дефференциальных уравнений в частных производных по фукнциям регулярных в иросмраисмвехммх переменных. Выводится приближенная зависимость для представления поля жидкости, Зто поле, вместе, с приближением плоской волны, используется для получения приближенных решений поведения оболочки. Цаются зкстенсивные численные результаты для смальных оболочек в морской воде.